Electrode Modification from the Electrolysis of $[M(Bipyridine)_3](ClO_4)_2$ ($M = Co^{II}$, Fe^{II}, and Ru^{II}) in Media of Low Dielectric Constant. Electrocatalytic Behavior and an Amperometric C_{60} Sensor

Krzysztof Winkler,[†] David A. Costa,[‡] Akari Hayashi,[‡] and Alan L. Balch*[,‡]

Department of Chemistry, University of California, Davis, California 95616, and Institute of Chemistry, University of Bialystok, Bialystok, Poland

Received: March 12, 1998; In Final Form: July 31, 1998

The voltammetric behavior of transition metal complexes of 2,2′-bipyridine, $[M^{II}(bpy)_3](ClO_4)_2$ ($M^{II} = Co^{II}$, Fe^{II}, or Ru^{II}), in toluene/acetonitrile mixtures has been studied by cyclic voltammetry. In solutions with a low acetonitrile-to-toluene ratio and tetra(*n*-butyl)ammonium perchlorate as supporting electrolyte, oxidation of $[M^{II}(bpy)_3](ClO_4)_2$ leads to the precipitation of a solid, electrochemically inactive phase of $[M^{III}(bpy)_3](ClO_4)_3$ (M = Co or Fe) on the electrode. Electrodes modified by this solid phase are shown to display catalytic waves that result from chemical reduction of the film by soluble species: $[M(bpy)_3]^+$ when no other electroactive species is present or $[C_{60}]^-$ when C_{60} is also present in the solution. The redox behavior of C_{60} on an electrode covered by a $[Co^{III}(bpy)_3](ClO_4)_3$ layer was extensively investigated. The catalytic current associated with the reduction of C_{60} at a $[Co^{III}(bpy)_3](ClO_4)_3$ modified electrode can be used for the quantitative determination of fullerene concentration in solution. The reduction current associated with square wave voltammetric experiments increased linearly with the concentration of C_{60} in the range of 0.25−20 μM. The detection limit is 0.1 μM. This method of fullerene quantitative determination exhibits good reproducibility, simplicity, and is relatively fast. Electrochemical oxidation of $[Ru^{II}(bpy)_3](ClO_4)_2$ does not produce an analogous redox inactive layer of $[Ru^{III}(bpy)_3](ClO_4)_3$.

Introduction

Recent work from this laboratory has utilized two component electrochemical procedures to generate polymeric fullerene films that adhere to a variety of electrode surfaces.[1,2] Such films have been obtained from the electroreduction of C_{60} or C_{70} in the presence of limited amounts of dioxygen, and related films are generated from the electroreduction of the epoxide $C_{60}O$.[1,3,4] The films obtained in this manner are likely to involve covalent C−O−C linkages, which are similar to those in $C_{120}O$,[5] and these linkages form the polymeric network that contributes to the films' general insolubility in organic solvents. Another class of films is formed by the reduction of C_{60} in the presence of transition metal complexes such as bis(benzonitrile)palladium(II)dichloride, $Ir(CO)_2Cl$(*p*-toluidine), and tris(pyridine)rhodium(III)trichloride.[2] In this group of films, covalent C_{60}−M−C_{60} linkages are likely to be present.[6] As a part of this work, we had occasion to examine the electrochemistry of C_{60} in the presence of $[Co^{II}(bpy)_3](ClO_4)_2$ and observed the results described here.

The electrochemistry of $[Co^{II}(bpy)_3]^{2+}$ and analogous bpy complexes with different metal ions has been previously documented.[7,8] In solution this cation undergoes a reversible, one-electron reduction and also a reversible, one-electron oxidation. The reduction is followed by a second reduction which appears to involve two electrons. Complexes such as $[Co^{II}(bpy)_3]^{2+}$ and related bpy complexes have been incorporated into a number of different chemically modified electrodes through covalent attachment, ion exchange, or polymerization.[9−12]

The electrochemical behavior of C_{60} has also received considerable attention. Up to six reversible, one-electron reduction steps have been observed,[13,14] while only one, reversible oxidation step, at quite positive potential, has been detected.[15] This well defined electrochemistry could be coupled with highly selective electrochemical techniques to produce a very powerful sensor for fullerene detection. To date only one paper has proposed the use of electrochemical methodology for detection of fullerenes. Kadish and co-workers applied fast scan-rate cyclic voltammetry at a microelectrode as a detection technique to monitor the separation of fullerenes by HPLC.[16] With ultramicroelectrodes the ohmic drop is reduced allowing for the performance of electrochemical measurements in very low dielectric constant solutions.

The results presented here describe a novel electrode modification with $[Co^{II}(bpy)_3](ClO_4)_2$ through simple precipitation that produces a sensor that can be used for quantitative fullerene detection and has potential applications for the detection of other redox-active species.

Results and Discussion

Electrochemical Behavior of $[Co^{II}(bpy)_3](ClO_4)_2$ in Acetonitrile/toluene Mixtures. The effects of changes in the ratio of acetonitrile to toluene on the electrochemical behavior of $[Co^{II}(bpy)_3](ClO_4)_2$ (with tetra(*n*-butyl)ammonium perchlorate as supporting electrolyte) are shown in Figure 1. If the amount of acetonitrile in the mixture is relatively high as it is in trace a (the acetonitrile/toluene ratio is 3/2 v/v), two reversible, one-electron redox processes (O_1/R_1) and (R_2/O_2) are observed. This behavior is consistent with the previous results obtained for this complex in acetonitrile solution with tetra(ethyl)ammonium

[†] University of Bialystok.
[‡] University of California.

10.1021/jp9814707 CCC: $15.00
Published on Web 11/10/1998

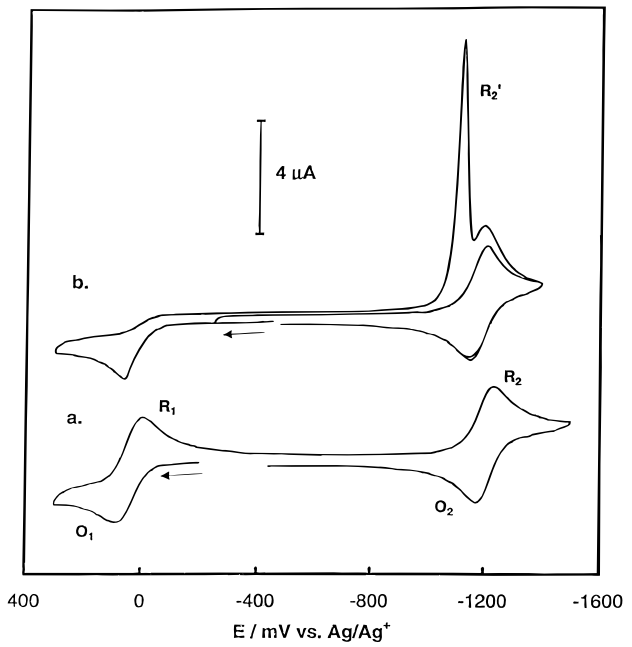

Figure 1. Cyclic voltammograms of solutions of 0.4 mM [Co^{II}(bpy)$_3$](ClO$_4$)$_2$ and 0.10 M TBAP in (a) 3/2 v/v toluene/acetonitrile and (b) 4/1 v/v toluene/acetonitrile. The sweep rate was 100 mV/s.

perchlorate as supporting electrolyte. Increasing of the percentage of toluene in the toluene/acetonitrile mixture results in significant changes of the voltammogram. Trace b of Figure 1 shows the voltammogram recorded in a solution with a 4:1 ratio of toluene to acetonitrile. The concentration of [Co^{II}(bpy)$_3$](ClO$_4$)$_2$ in this mixture is very close to that of a saturated solution. The oxidation of [Co^{II}(bpy)$_3$]$^{2+}$ is still observed at potentials close to 0 V, but the expected reduction peak (R_1) is not recorded in the subsequent cathodic scan. Additionally, in the potential range of the [Co^{II}(bpy)$_3$]$^{2+}$ reduction (about −1200 mV), a new, sharp peak (R_2') is observed. The R_2' peak is not observed if the anodic switching potential is less positive than the oxidation potential of [Co^{II}(bpy)$_3$]$^{2+}$. In that case, as seen in the inner part of trace b, a totally reversible diffusion controlled process is observed for the reduction of the [Co^{II}(bpy)$_3$]$^{2+}$. These data suggest that the R_2' peak is related to changes in the electrode surface that occur in the potential range of the oxidation of [Co(bpy)$_3$]$^{2+}$.

The oxidation of [Co^{II}(bpy)$_3$](ClO$_4$)$_2$ and its influence on the subsequent reduction was investigated in more detail. The multicyclic voltammogram recorded in the potential range from −600 to 300 mV is shown in trace a of Figure 2. The oxidation current recorded for the first cycle is shifted toward more positive potentials compared to the currents recorded for the second and following cycles, and there is a gradual decline in the current in later cycles. These results also strongly suggest that the oxidation of [Co^{II}(bpy)$_3$]$^{2+}$ in the 4:1 toluene/acetonitrile is accompanied by formation of a solid phase on the electrode surface. Thus, in this low dielectric constant medium the insoluble salt, [Co^{III}(bpy)$_3$](ClO$_4$)$_3$, precipitates on the electrode surface. Indeed, optical microscopic examination of the electrode following anodic oxidation reveals the presence of a microcrystalline deposit on the electrode surface. A scanning electron micrograph of the electrode after oxidative treatment as described above is shown in Figure 3. Crystallites up to 7 μm long are apparent on the surface.

The amount of [Co^{III}(bpy)$_3$](ClO$_4$)$_3$ deposited on the electrode surface affects the current associated with the reduction of the [Co^{II}(bpy)$_3$]$^{2+}$. Trace b of Figure 2 presents voltammograms

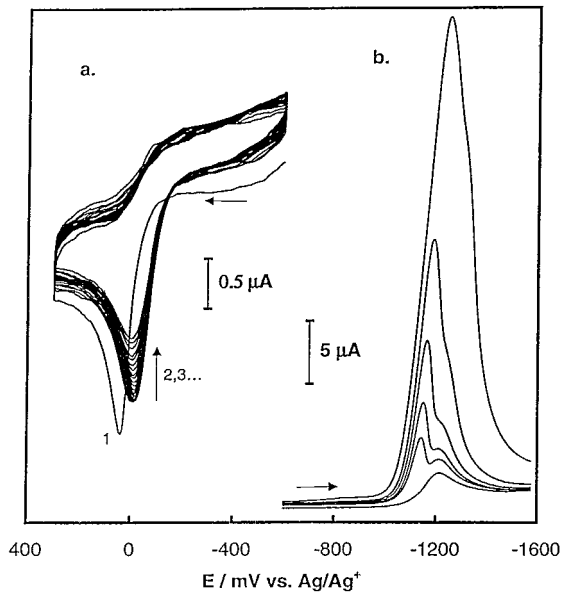

Figure 2. (a) Multicyclic voltammograms (25 cycles) of 0.4 mM [Co^{II}(bpy)$_3$](ClO$_4$)$_2$ in toluene/acetonitrile (4/1 v/v) containing 0.10 M TBAP. The sweep rate was 100 mV/s. (b) Voltammograms of 0.3 mM [Co^{II}(bpy)$_3$](ClO$_4$)$_2$ in toluene/acetonitrile (4/1 v/v) containing 0.10 M TBAP with the electrode modified by electrolysis at 300 mV for 0 s, 1, 2, 5, 15, and 45 s. The sweep rate was 100 mV/s.

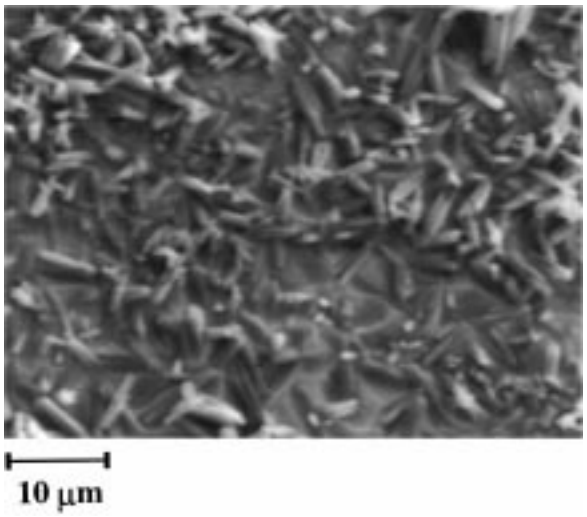

Figure 3. Scanning elelectron micrograph of a gold electrode after oxidation in a toluene/acetonitrile (4/1 v/v) solution of [Co^{II}(bpy)$_3$](ClO$_4$)$_2$ and 0.10 M TBAP

recorded for differing degrees of surface modification. The gold electrode surface was initially modified under potentiostatic conditions at 300 mV for a predetermined time period that varied from 1 to 45 s. From Figure 2b it is apparent that the growth of the R_2' peak depends on the length of time utilized for electrode modification (and presumably the amount of material deposited on the electrode surface).

The voltammetric behavior of a 0.45 mM solution of [Co^{II}(bpy)$_3$](ClO$_4$)$_2$ in toluene/acetonitrile (4/1 v/v) depends on both the sweep rate and the concentration of the reactant. In Figure 4 the effects of the sweep rate on the electrochemical oxidation and reduction of [Co^{II}(bpy)$_3$]$^{2+}$ are shown. At higher sweep rates, reduction of the product formed during the oxidation of the complex is observed. The sharp and symmetrical shape of the R_1 peak suggests that a surface process is involved in this electrode reaction. The ratio of the charge corresponding to the anodic and cathodic processes, O_1/R_1, is

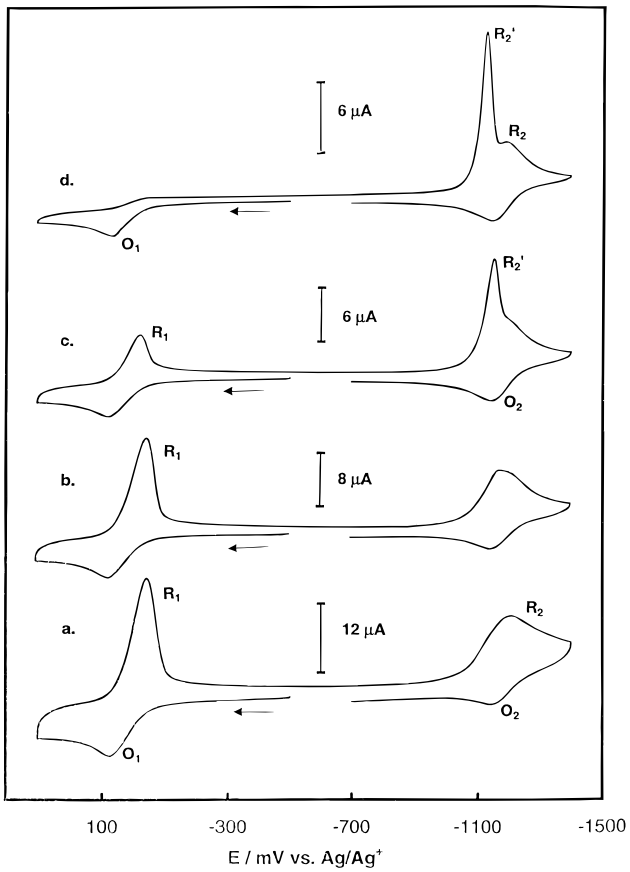

Figure 4. Cyclic voltammograms of 0.45 mM $[Co^{II}(bpy)_3](ClO_4)_2$ in toluene/acetonitrile (4/1 v/v) containing 0.10 M TBAP. The sweep rate was (a) 2000 mV/s, (b) 1000 mV/s, (c) 500 mV/s, and (d) 100 mV/s.

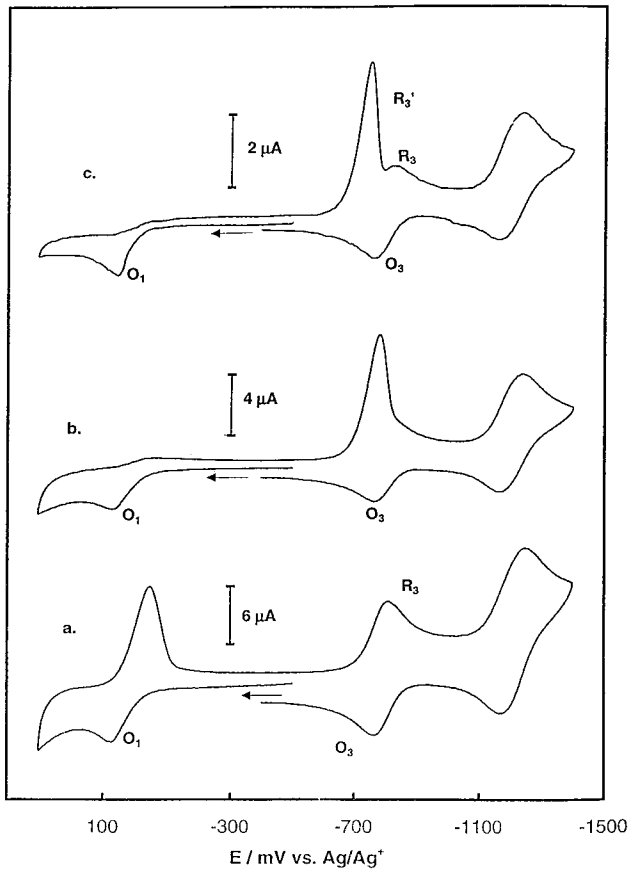

Figure 5. Cyclic voltammograms of 0.4 mM $[Co^{II}(bpy)_3](ClO_4)_2$ and 0.25 mM C_{60} in toluene/acetonitrile (4/1 v/v) containing 0.10 M TBAP. The sweep rate was (a) 2000 mV/s, (b) 500 mV/s, (c) 100 mV/s.

SCHEME 1

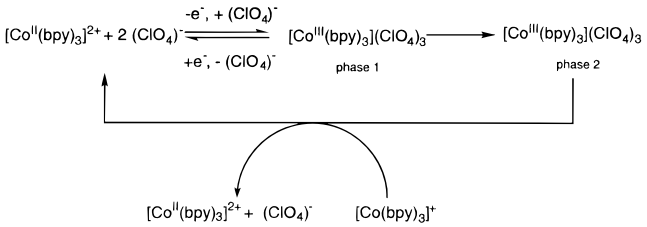

almost equal to unity (0.91) for a sweep rate 1000 V/s. This ratio decreases with decreasing sweep rate. Finally, for a sweep rate of 100 mV/s practically no reduction current was observed in the potential range close to 0 V. Changes in the R_2' peak with sweep rate correlate well with those observed for the R_1 peak. At a high sweep rate (1000 mV/s), the reduction peak R_2 is only slightly distorted by the presence of the R_2' reduction current at a slightly less negative potential. With a decrease in the sweep rate, the formation of the peak, R_2', is observed, and this feature becomes prominent in traces c and d. The electrochemical behavior of $[Co^{II}(bpy)_3]^{2+}$ also depends on the concentration of the reactant. Thus, in a 0.05 mM solution of $[Co^{II}(bpy)_3]^{2+}$, reversible electrochemical behavior was observed both for the oxidation and reduction processes even for slow sweep rates.

The results presented above indicate that a solid-phase deposition process is associated with the electrochemical oxidation of $[Co^{II}(bpy)_3]^{2+}$ in low dielectric constant media as shown in Scheme 1. The initially formed phase of $[Co^{III}(bpy)_3](ClO_4)_3$ (phase 1 in Scheme 1) is electrochemically active and can be reduced in the cathodic cycle. The rearrangement of this layer results in the formation of an electrochemically inactive solid deposit. (phase 2 in Scheme 1). Phase 2 can be reduced by $[Co^{I}(bpy)_3]^{+}$ that is formed in solution by reduction of $[Co^{II}(bpy)_3]^{2+}$. This process gives rise to the catalytic wave, R_2'.

Electrochemical Reduction of C_{60} at an Electrode Covered by a Layer of $[Co(bpy)_3](ClO_4)_3$. Figure 5 shows cyclic voltammograms at three different sweep rates for a solution that contains both $[Co^{II}(bpy)_3](ClO_4)_2$ and C_{60}. The potential of the first reduction step for C_{60} (R_3/O_3) is less negative than the potential of the reduction of $[Co^{II}(bpy)_3]^{2+}$. However, the formal potentials of the $[C_{60}]^{-1/-2}$ redox couple and the $[Co(bpy)_3]^{2+/1+}$ redox couple are almost the same. Thus the currents recorded at potentials more negative than −1100 mV are the sums of the currents for reduction of $[C_{60}]^{-}$ and of $[Co^{II}(bpy)_3]^{2+}$. For the voltammograms shown in Figure 5, the potential was initially swept in the positive direction in order to oxidize $[Co^{II}(bpy)_3]^{2+}$ and to form a deposit of $[Co^{III}(bpy)_3](ClO_4)_3$ on the electrode surface. Trace a shows the behavior at a high sweep rate where the $[Co^{III}(bpy)_3](ClO_4)_3$ layer was completely reduced during the cathodic sweep. Consequently, both chemically and electrochemically reversible reductions were recorded at negative potentials. For lower sweep rates as seen in traces b and c, the diffusion-controlled reduction peak of C_{60} is preceded by a new, sharp peak (R_3'). This feature resembles that seen at a more negative potential in the solution containing $[Co^{II}(bpy)_3]^{2+}$ only (traces c and d of Figure 4). In the cases with Traces b and c of Figure 5, reduction of $[Co^{II}(bpy)_3]^{2+}$ at potentials more negative than −1100 mV is not altered even though a layer of $[Co^{III}(bpy)_3](ClO_4)_3$ was initially deposited. The comparison of the features labeled R_2' in Figures 1 and 3 and R_3' in Figure 5 peaks suggests that the

SCHEME 2

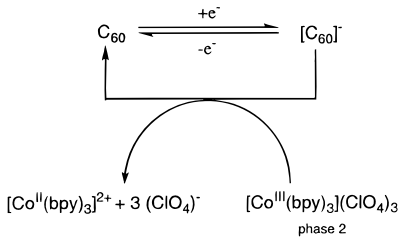

chemical nature of the processes responsible for the formation of these peaks is similar.

The behavior shown in Figure 5 can be explained by assuming that a redox reaction between $[C_{60}]^-$ and $[Co^{III}(bpy)_3](ClO_4)_3$ allows the salt to be removed from the electrode through reduction, and that under the conditions of this experiment, the rate of this reaction is sufficient to allow all of the surface layer of $[Co^{III}(bpy)_3](ClO_4)_3$ to be removed through reduction with $[C_{60}]^-$. Hence in Figure 5, the peak R_2' is absent; although it is seen in Figures 1 and 3. The large difference in the formal potentials of $[Co(bpy)_3]^{3+/2+}$ redox couple and the $[C_{60}]^{0/-1}$ redox couple favors this chemical process. For this system the catalytic process shown in Scheme 2 operates to continually regenerate C_{60} from $[C_{60}]^-$. This regeneration causes the dramatic growth of the peak R_3' that is seen in Figure 5. The absence of a peak corresponding to peak R_2' at ca -1100 mV in Figure 5 is a simple consequence of the relatively high concentration of C_{60} used in this experiment. In these experiments the C_{60} concentration is high enough and the mass of the $[Co^{III}(bpy)_3](ClO_4)_3$ layer is small enough so that the layer of the oxidized cobalt complex is completely removed by the catalytic process shown in Scheme 2.

$[Co^{III}(bpy)_3](ClO_4)_3$ Coated Electrode as an Amperometric Sensor for C_{60}. If the amount of the $[Co^{III}(bpy)_3](ClO_4)_3$ layer on the electrode surface is large and the concentration of C_{60} in the solution is low, then the solid phase may not be completely reduced by the $[C_{60}]^-$ that is formed during C_{60} reduction. In this case the magnitude of C_{60} reduction catalytic current should be controlled by the concentration of fullerene in the solution, and then this system can be used for quantitative determination of C_{60}.

The voltammograms obtained in a toluene/acetonitrile (4:1 v/v) mixtures containing different C_{60} concentrations (in the micromolar range) along with a fixed concentration (0.45 mM) of $[Co^{II}(bpy)_3](ClO_4)_2$ are shown in Figure 6. In trace a after deposition of the $[Co^{III}(bpy)_3](ClO_4)_3$ layer, a broad plateau is observed in the cathodic sweep at ca -800 mV and a catalytic spike is seen at -1100 mV. The shape of this feature is similar to those seen for a homogeneous catalytic process of the type E_rC_i' with a fast chemical reaction that follows the charge-transfer step.[17,18] In Traces b and c the first cathodic cycles were recorded at an electrode free from the solid layer of $[Co^{III}(bpy)_3](ClO_4)_3$. Since the fullerene concentration was 2 orders of magnitude lower than the concentration of the cobalt complex, no current was observed in the potential range of C_{60} reduction for these traces. However, once the electrode was coated with $[Co^{II}(bpy)_3](ClO_4)_3$ by sweeping to 200 mV, the voltammograms show two new features on the next sweep to negative potentials. The broad feature emerges at ca. -800 mV and the sharp spike R_2' emerges prior to the reduction of $[Co^{II}(bpy)_3]^{2+}$. The presence of the peak R_2' indicates that the solid layer of $[Co^{III}(bpy)_3](ClO_4)_3$ is not completely reduced by $[C_{60}]^-$ when the concentration of C_{60} is low.

Despite the observations shown in Figure 6, cyclic voltammetry is not the optimum technique for quantitative determination of fullerene concentration in solution. The current of the plateau at about -800 mV is not suitably reproducible even if the signal-to-noise ratio (variance from the background current) is higher than 3. However, a linear relationship between the limiting electrocatalytic current for C_{60} reduction by dc voltammetry and fullerene concentration in solution was observed for C_{60} concentrations between 2 and 50 μM.

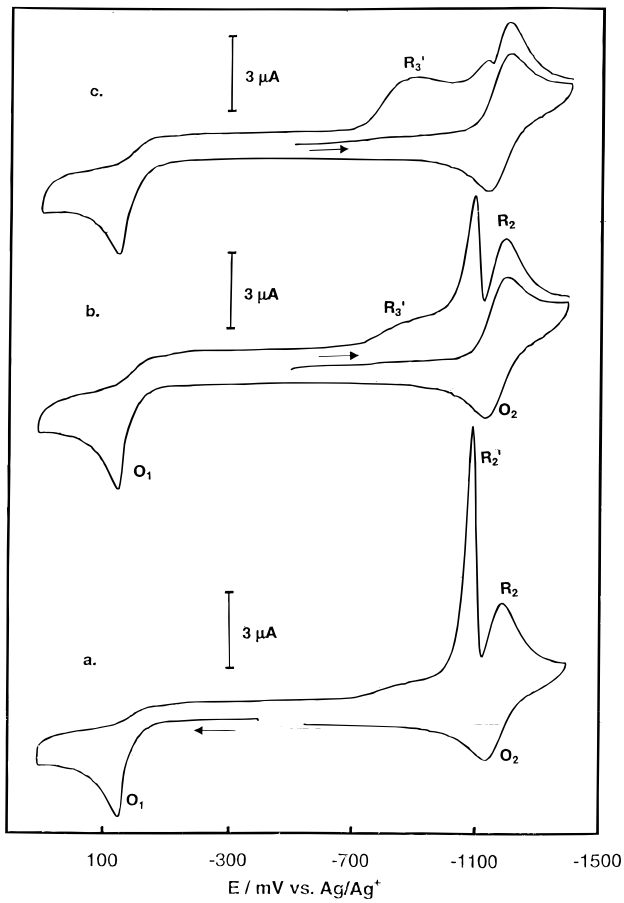

Figure 6. Cyclic voltammograms of 0.45 mM $[Co^{II}(bpy)_3](ClO_4)_2$ and (a) 0.2 μM C_{60}, (b) 0.4 μM C_{60}, and (c) 1 μM C_{60} in toluene/acetonitrile (4/1 v/v) containing 0.10 M TBAP. The sweep rate was 100 mV/s.

To increase the sensitivity and precision for the quantitative determination C_{60} concentrations, Osteryoung square wave voltammetry was used for a toluene/acetonitrile solutions that contained both C_{60} and $[Co^{II}(bpy)_3](ClO_4)_2$ along with the supporting electrolyte. The procedure involved initial deposition of a layer of $[Co^{III}(bpy)_3](ClO_4)_3$ on the electrode through oxidation at 300 mV for 2 s followed by recording the voltammogram. After electrode pretreatment, the square wave voltammogram obtained from a solution containing 4 μM C_{60} and 0.45 mM $[Co^{II}(bpy)_3](ClO_4)_2$ is shown in trace a of Figure 7. Four reductive processes are observed. Peak R_1 results from the partial reduction of the layer of $[Co^{III}(bpy)_3](ClO_4)_3$. Peak R_3' is due to the electrocatalytic reduction of C_{60} according to Scheme 2. This peak was used for the quantitative determination of C_{60} in the toluene/acetonitrile mixture. Peak R_2 is due to the reduction of $[Co(bpy)_3]^{2+}$ in solution, and it is preceded by the electrocatalytic peak R_2', which is due to electrocatalytic reduction of the $[Co^{III}(bpy)_3](ClO_4)_3$ film by the process shown in Scheme 1. Part b of Figure 7 shows the growth of the height of the peak R_3' with increasing concentration of C_{60} in solution.

Figure 8 shows a plot of the peak current for the process R_3' versus the C_{60} concentration from data analogous to those shown

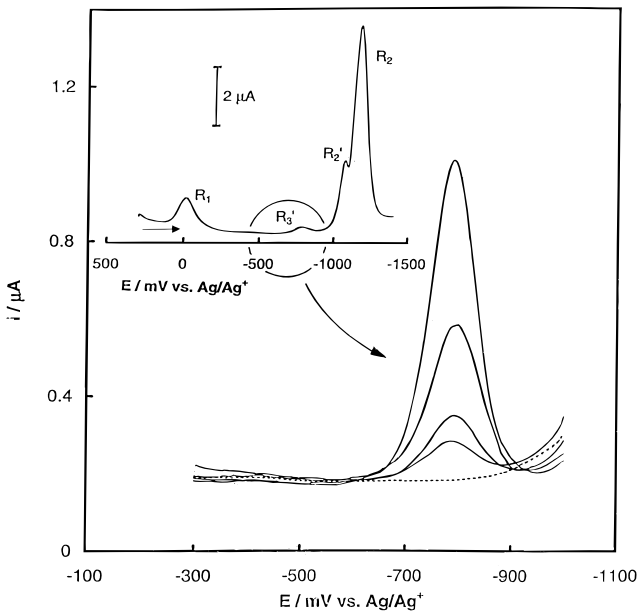

Figure 7. (a) Osteryoung square wave voltammogram of 0.45 mM $[Co^{II}(bpy)_3](ClO_4)_2$ and 4 μM C_{60} in toluene/acetonitrile (4/1 v/v) containing 0.10 M TBAP. (b) The Osteryoung square wave peak for catalytic electroreduction of C_{60} obtained for different fullerene concentrations (1, 2, 4, and 8 μM). The broken line indicates the background current obtained in the absence of C_{60} in solution. The potential step was 4 mV, the square wave amplitude was 25 mV, the square wave frequency was 15 Hz, the quiet time was 2 s.

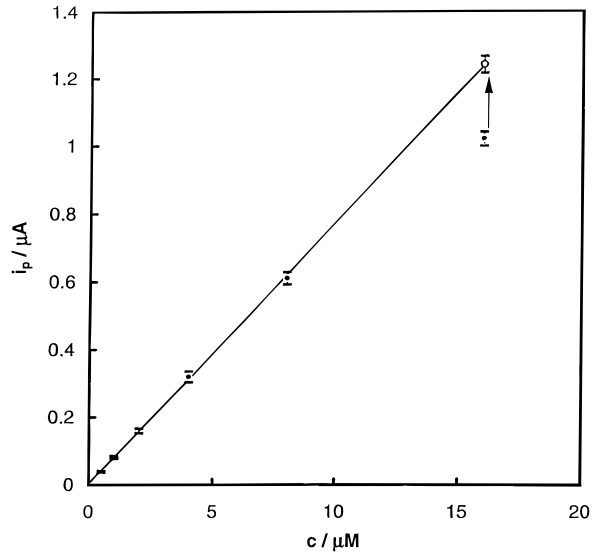

Figure 8. A plot of peak current (i_p) versus the C_{60} concentration from data like those shown in Figure 6 for the electrocatalytic reduction of C_{60} on an electrode coated with $[Co^{III}(bpy)_3](ClO_4)_3$.

in Figure 7. This plot is linear with a slope of 0.077(1) μA/μM, an intercept of 0.0039(12) μA, and a correlation coefficient of 0.9997. Each point on this calibration curve was calculated from the average value of five successive measurements. Above 15 μM the relation between the peak current and concentration deviates from linearity. This is ascribed to the complete reduction of the $[Co^{III}(bpy)_3](ClO_4)_3$ layer from the electrode surface, and at that concentration of C_{60} the peak R_2' is not observed. However, if the amount of the solid phase deposited on the electrode is increased by increasing the time for oxidative deposition at 300 mV, the linear dependence is extended as shown by open point in Figure 8. A C_{60} detection limit of 0.2 μM was obtained with this procedure with a signal-to-noise ratio

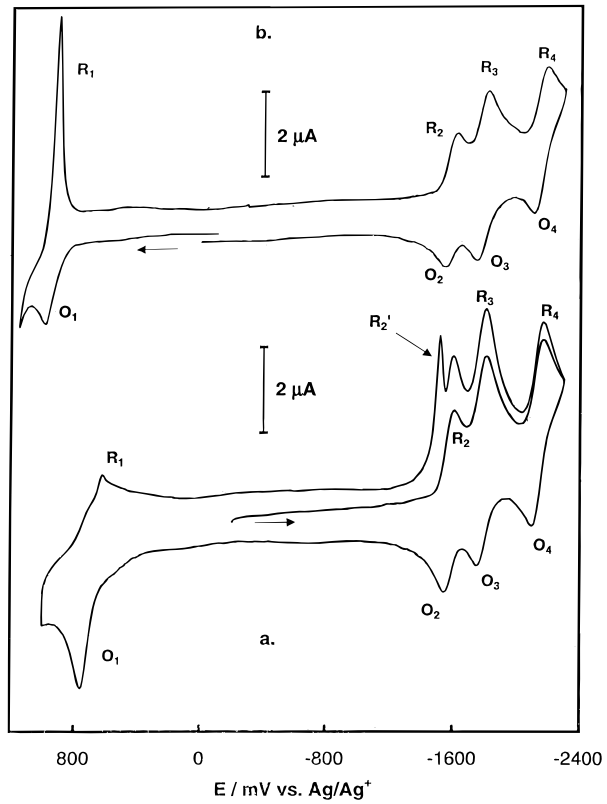

Figure 9. (a) Cyclic voltammogram of 0.4 mM $[Fe^{II}(bpy)_3](ClO_4)_2$ in a toluene/acetonitrile (4/1 v/v) mixture containing 0.10 M TBAP. (b) Cyclic voltammogram of 0.38 mM $[Ru^{II}(bpy)_3](ClO_4)_2$ in a toluene/acetonitrile (4/1 v/v) mixture containing 0.10 M TBAP. The sweep rate was 100 mV/s.

of 3. The C_{60} concentration was also repeatedly determined (20 times) for 0.5 and 4.0 μM solutions of C_{60} with relative standard deviations of 3.5% and 2.0%, respectively.

Electrocatalytic Currents from $[Fe^{II}(bpy)_3](ClO_4)_2$ and $[Ru^{II}(bpy)_3](ClO_4)_2$. The electrochemical behavior of $[Fe^{II}(bpy)_3](ClO_4)_2$ and $[Ru^{II}(bpy)_3](ClO_4)_2$ in the presence and absence of C_{60} were also investigated. Trace a of Figure 9 shows the voltammogramof a solution of $[Fe^{II}(bpy)_3](ClO_4)_2$ in toluene/acetonitrile (4/1 v/v). For the first cathodic scan recorded at the clean electrode surface, three reversible reduction peaks, R_2(Fe), R_3(Fe), and R_4(Fe), are observed. These peaks are due to the successive, one-electron reductions of $[Fe^{II}(bpy)_3]^{2+}$.[8] In the positive-going scan, the oxidation of $[Fe(bpy)_3]^{2+}$, O_1(Fe), takes place at a potential more positive than about 600 mV. The fact that the ratio of the height of the cathodic, R_1(Fe), to anodic, O_1(Fe), peak currents is significantly lower than 1 indicates that oxidation is accompanied by the formation of solid $[Fe^{III}(bpy)_3](ClO_4)_3$ on the electrode surface. Therefore, in the second cathodic cycle, the electrode is covered by the solid layer of $[Fe(bpy)_3](ClO_4)_3$, and upon rereduction a sharp peak, R_2'(Fe), appears in voltammogram at a less negative potential than the R_2(Fe) peak. Overall, the behavior shown here is analogous to that seen for $[Co^{II}(bpy)_3](ClO_4)_2$ (see trace b of Figure 1). Trace b of Figure 9 shows the voltammogram of a solution of $[Ru^{II}(bpy)_3](ClO_4)_2$ in toluene/acetonitrile (4/1 v/v).

Figure 10 shows electrochemical data obtained from a toluene/acetonitrile solution that contains a mixture of C_{60} and $[Fe^{II}(bpy)_3](ClO_4)_2$. Trace a shows the cyclic voltammogram. In the initial reductive cycle with a clean electrode, the reversible reduction of C_{60} is followed by the first, one-electron reduction of $[Fe^{II}(bpy)_3]^{2+}$. In the subsequent anodic sweep, a layer of $[Fe^{III}(bpy)_3](ClO_4)_3$ is deposited, and in the second cathodic

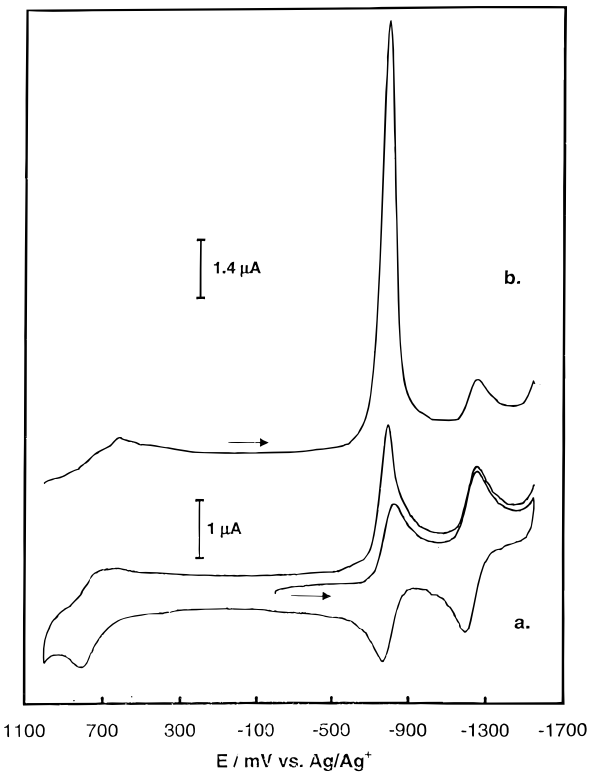

Figure 10. (a) Cyclic voltammogram of 0.3 mM $[Fe^{II}(bpy)_3](ClO_4)_2$ and 0.3 mM C_{60} in toluene/acetonitrile (4/1 v/v) mixture containing 0.10 M TBAP. Sweep rate was 100 mV/s. (b) Voltammogram of 0.3 mM $[Fe^{II}(bpy)_3](ClO_4)_2$ and 0.3 mM C_{60} in toluene/acetonitrile (4/1 v/v) mixture containing 0.10 M TBAP recorded at the electrode modified at potential 1000 mV for 30 s. The sweep rate was 100 mV/s.

cycle an enhanced peak is observed at −850 mV due to the electrocatalytic reaction that uses $[C_{60}]^-$ to reduce the film. In trace b of Figure 10 the dc voltammogram for this same solution after pretreatment of the electrode at 1000 mV for 30 s is shown. Three reductive processes are seen: the direct reduction of the $[Fe^{III}(bpy)_3](ClO_4)_3$ film, the electrocatalytic reduction of C_{60}, and the second, one-electron reduction of C_{60}.

The voltammogram recorded in a toluene/acetonitrile (4:1 v/v) solution of $[Ru^{II}(bpy)_3](ClO_4)_2$ is shown in trace b of Figure 9. For this system, the deposit of $[Ru^{III}(bpy)_3](ClO_4)_3$ formed on the electrode surface during the oxidative cycle is electrochemically active. The sharp surface peak (R_1) at about 910 mV is responsible for the reduction of the surface precipitate of $[Ru^{III}(bpy)_3](ClO_4)_3$. Such reversible behavior was observed for both high and low sweep rates. Also, the precipitation of the salt on the electrode surface at potentials more positive than 1000 mV does not result in the formation of an electrochemically inactive layer on the electrode. Consequently no electrocatalytic currents are observed on the cathodic cycle shown in trace b of Figure 9.

Conclusions

By operating in a medium that poorly solvates trications, gold electrodes are modified through simple precipitation of $[M^{III}(bpy)_3](ClO_4)_3$ ($M = Co^{III}$, Fe^{III}, or Ru^{III}) during the anodic oxidation of $[M^{II}(bpy)_3](ClO_4)_2$. The solid films of $[Co^{III}(bpy)_3](ClO_4)_3$ and $[Fe^{III}(bpy)_3](ClO_4)_3$ become electrochemically inactive and this is ascribed to a phase change. A reviewer has suggested that this may be due to hydrolysis of the complex cations to form the μ-oxo dimer, $[(bpy)_2M^{III}OM^{III}(bpy)_2](ClO_4)_4$.[19] Indeed such a chemical reaction involving adventitious water and the surface of the microcrystals of $[M^{III}(bpy)_3](ClO_4)_3$ could serve to passivate the deposit against electrochemical reduction. The resulting electrodes show catalytic waves that result from the chemical reduction of the deposit of $[M^{III}(bpy)_3](ClO_4)_3$ which otherwise cannot be reduced via electron transfer directly from gold. These catalytic waves can be produced by electrogeneration of $[M(bpy)_3]^+$ or by electrogeneration of a species such as $[C_{60}]^-$ which is introduced into the system from a second source. The catalytic electroreduction with C_{60} has been developed into a sensitive sensor for C_{60}.

A number of methods have been developed to modify electrodes with complexes related to $[M^{II}(bpy)_3]^{2+}$.[9−12] The electrochemical polymerization of vinylpyridine and vinylbipyridine metal complexes has been extensively studied.[20−23] The mechanisms of charge storage within these polymerized films, and electron-transfer processes involved with the electrochemical behavior of these films have also received significant scrutiny.[24−30] It is important to note that the behavior described in the present manuscript is distinct from that occurring in polymerized films derived from vinyl monomers. For such polymer-coated electrodes, the electrode surface ideally should remain intact throughout any electrochemical process. For the behavior we describe here however, the cycle of precipitation and dissolution is critical to the electrochemical processes.

The method of quantitative determination of C_{60} based on the electrocatalytic effect shows relatively high sensitivity and very good reproducibility. In our work C_{60} was chosen as a model system for study. However, this technique can be developed to allow the quantitative determination of other fullerenes and their derivatives, as well. It should also be useful for detecting other reversible redox systems with formal potentials more cathodic that the formal potential of the $[M(bpy)_3]^{3+/2+}$ redox couple in low dielectric constant solutions, and preliminary results in this laboratory indicate that other reversible redox systems do produce similar catalytic waves. With the present method, the detection limit for C_{60} is more than an order of magnitude lower that the detection limit of UV−vis spectroscopy or fast cyclic voltammetry at ultramicroelectrodes.[16] It is expected that utilization of ultramicroelectrodes will allow the sensitivity of this method to be significantly increased. It is also important to note that the method is relatively fast. It takes only a few second to cover an electrode by the layer of $[M^{III}(bpy)_3](ClO_4)_3$.

The fact that the solid layer is dissolved during the reduction by $[C_{60}]^-$ is a somewhat of a disadvantage of this method. This problem may limit its application to the study of the concentration of fullerenes in flow systems. However, the solid layer is also easily regenerated from readily available metal complexes without further chemical or electrochemical processing.

Experimental Section

The C_{60} was purchased from MER Corp., Tucson, AZ, and used without additional purification. Tetra(*n*-butyl)ammonium perchlorate (TBAP) (Sigma Chemical Co.) was dried under reduced pressure at 70 °C for 24 h. The transition metals salts, $[Co^{II}(bpy)_3](ClO_4)_2$,[31] $[Fe^{II}(bpy)_3](ClO_4)_2$,[31] and $[Ru^{II}(bpy)_3](ClO_4)_2$[32] were prepared according to procedures described in the literature. Acetonitrile (99.8%) was used as received from Aldrich. Toluene (Aldrich Chemical Co.) was purified by distillation over sodium under an argon atmosphere.

Voltammetric experiments were performed using a BAS CV50-W Electroanalytical System with a three electrode cell. The working electrode was a gold disk (Bioanalytical Systems, Inc.) with a diameter of 1.5 mm. Prior to the experiment, the

electrode was polished with a fine carborundum paper and then with a 0.5 μm alumina slurry. Next the electrode was sonicated in water in order to remove the traces of alumina from the gold surface, washed with water, and dried. A silver wire that was immersed in 0.01 M silver perchlorate and 0.09 M TBAP in acetonitrile and separated from the working electrode by a ceramic tip (Bioanalytical Systems, Inc.) served as the reference electrode. With this reference electrode in a 4:1 toluene/acetonitrile solution, the ferrocene/ferrocinium redox potential was +161 mV. All potentials are expressed with respect to this electrode. The counter electrode was a platinum tab with an area of $\sim$0.5 cm^2.

Scanning electron micrograph images were obtained with the use of an ISI (Topcon) DS 130 microscope with a LaB_6 crystal filament. The accelerating voltage of the electron beam was 10 kV.

Acknowledgment. We thank the National Science Foundation (Grant CHE-9610507) for financial support.

References and Notes

(1) Winkler, K.; Costa, D. A.; Fawcett, W. R.; Balch, A. L. *Adv. Mater.* **1997**, *9*, 153.

(2) Balch, A. L.; Costa, D. A.; Winkler, K. *J. Am. Chem. Soc*. **1998**, *120*, 9614.

(3) Fedruco, M.; Costa, D. A.; Balch, A. L.; Fawcett, W. R. *Angew. Chem., Int. Ed. Engl.* **1995**, *34*, 194.

(4) Winkler, K.; Costa, D. A.; Balch, A. L.; Fawcett, W. R. *J. Phys. Chem*. **1995**, *99*, 17431.

(5) Smith, A. B.; Tokuyama, H.; Strongin, R. M.: Furst, G. T.; Romanow, W. J.; Chait, B. T.; Mirza, U. A.; Haller, I. *J. Am. Chem. Soc*. **1995**, *117*, 9359. Lebedkin, S.; Ballenweg, S.; Gross, J.; Taylor, R. *Tetrahedron Lett.* **1995**, *36* 4971. Balch, A. L.; Costa, D. A.; Fawcett, W. R.; Winkler, K. *J. Phys. Chem.* **1996,** *100*, 4823. Penn, S. G.; Costa, D. A.; Balch, A. L.; Lebrilla, C. B. *Int. J. Mass Spectrosc. Ion Processes* **1997**, *169/170*, 371.

(6) For a review on transition metal/fullerene chemistry, see: Balch, A. L.; Olmstead, M. M. *Chem. Rev*. **1998**, *98*, 2123.

(7) Willet, B. C.; Anson, F. C. *J. Electrochem. Soc*. **1982**, *129*, 1260.

(8) Richert, S. A.; Tsang, P. K. S.; Sawyer, D. T. *Inorg. Chem.* **1989**, *28*, 2471.

(9) Abruña, H, D. *Coord. Chem. Revs*. **1988**, *86*, 135.

(10) Wang, J. In *Electroanalytical Chemistry*, Bard, A. J., Ed.; Marcel Dekker: New York, 1989; Vol. 1, Chapter 1.

(11) Kelcher, K. *Electroanalysis* **1990**, *2*, 419.

(12) Gould, S.; Leasure, R. M.; Meyer, T. J. *Chem. Br*. **1995**, 891.

(13) Xie, Q.; Perez-Coroleroi, E.; Echegoyen, L. *J. Am. Chem. Soc.* **1992**, *114*, 3978.

(14) Ohsawa, Y.; Saji. T. *J. Chem. Soc., Chem. Commun*. **1992** 781.

(15) Xie, Q.; Arias, F.; Echegoyen, L. *J. Am. Chem. Soc.* **1993**, *115*, 9818.

(16) Soucaze-Guillous, B.; Kutner, W.; Kadish, K. M. *Anal. Chem.* **1993**, *65*, 669.

(17) Nicholson, R. S.; Shain, I. *Anal. Chem.* **1964**, *36*, 706.

(18) Bard, A. J.; Faulkner, L. R. *Electrochemical Methods*, J. Wiley and Sons: New York, 1980; p 455.

(19) Ehman, D. L.; Sawyer, D. S. *Inorg. Chem*. **1969**, *8*, 900.

(20) Denisevich, P.; Abruña, H. D.; Leidner, C. R.; Meyer, T. J.; Murray, R. W. *Inorg. Chem.* **1982**, *21*, 2153.

(21) Calvert, J. M.; Schmehl, R. H.; Sullivan, B. P.; Facci, J. S.; Meyer, T. J.; Murray, R. W. *Inorg. Chem.* **1983**, *22*, 2151.

(22) Surridge, N. A.; Keene, F. R.; White, B. A.; Facci, J. S.; Silver, M.; Murray, R. W. *Inorg. Chem.* **1990**, *29*, 4950.

(23) McCarley, R. L.; Thomas, R. E.; Irene, E. A.; Murray, R. W. *J. Electrochem. Soc.* **1990**, *137*, 1485.

(24) Facci, J. S.; Schmehl, R. H.; Murray, R. W. *J. Am. Chem. Soc.* **1982**, *104*, 4959.

(25) Leidner, C. R.; Murray, R. W. *J. Am. Chem. Soc.* **1984**, *106*, 1606.

(26) Jernigan, J. C.; Murray, R. W. *J. Phys. Chem.* **1987**, *91*, 2030.

(27) Zhang, H.; Murray, R. W. *J. Am. Chem. Soc.* **1991**, *113*, 5183.

(28) Surridge, N. A.; Zvanut, M. E.; Keene, F. R.; Sosnoff, C. S.; Silver, M.; Murray, R. W. *J. Phys. Chem.* **1992**, *96*, 962.

(29) Jernigan, J. C.; Murray, R. W. *J. Am. Chem. Soc.* **1990**, *112*, 1034.

(30) Coury, L. A., Jr.; Murray, R. W.; Johnson, J. L.; Rajagopalan, K. V. *J. Phys. Chem.* **1991**, *95*, 6034.

(31) Burstall, F. H.; Nyholm, R. S. *J. Chem. Soc*. **1952**, 3570.

(32) Burstall, F. H. *J. Chem. Soc*. **1938**, 173.